Palladium electrodissolution from model surfaces and nanoparticles

Enrico Pizzutilo[a*], Simon Geiger[a], Simon J. Freakley[b], Andrea Mingers[a], Serhiy Cherevko[a,c], Graham J. Hutchings[b], Karl J. J. Mayrhofer[a,c,d*]

[a]*Department of Interface Chemistry and Surface Engineering, Max-Planck-Institut für Eisenforschung GmbH, Max-Planck-Strasse 1, 40237 Düsseldorf, Germany*

[b]*Cardiff Catalysis Institute, School of Chemistry, Cardiff University, Main Building, Park Place, Cardiff, CF10 3AT*

[c]*Helmholtz-Institute Erlangen-Nürnberg for Renewable Energy (IEK-11), Forschungszentrum Jülich, Egerlandstr. 3, 91058 Erlangen, Germany*

[d]*Department of Chemical and Biological Engineering, Friedrich-Alexander-Universität Erlangen-Nürnberg, Egerlandstr. 3, 91058 Erlangen, Germany*

[*]*Corresponding authors: pizzutilo@mpie.de mayrhofer@mpie.de*
Tel.: +49 211 6792 160, FAX: +49 211 6792 218

SUPPORTING INFORMATION

1 Comparison of poly-Pd CVs in RDE and SFC

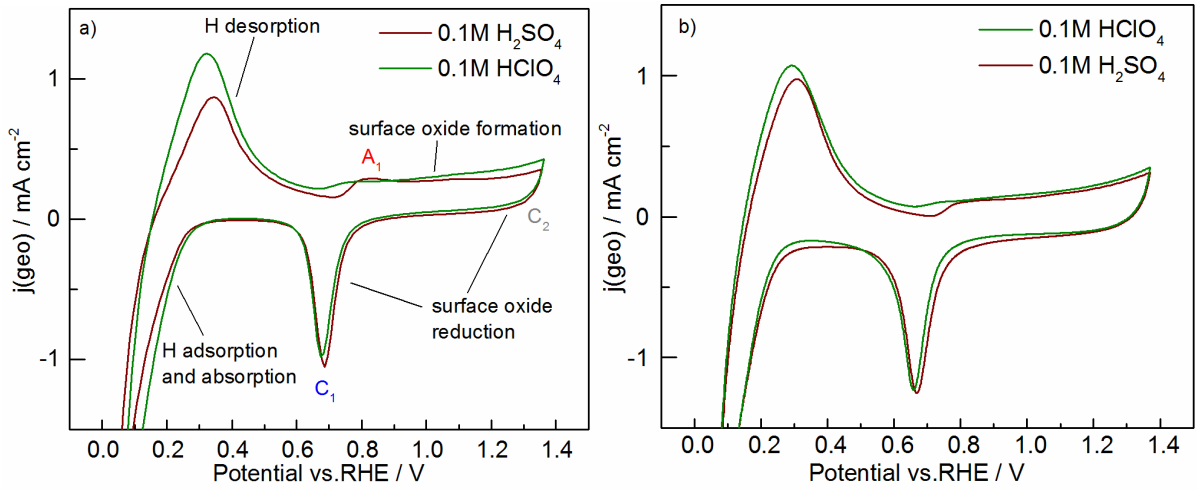

Figure S1 CVs taken on a poly-Pd electrode in the SFC(a) and RDE (b) setup in 0.1M $HClO_4$ and in 0.1M H_2SO_4. Scan rate: 200 mV s^{-1}.

Poly-Pd cyclic voltammogramms in deaerated solution (Figure S1) are recorded using RDE setup with perchloric and sulfuric acid. These CVs validate the results obtained with the SFC system (shown in Figure 1): classical poly-Pd features including H absorption and adsorption/desorption, Pd surface oxide formation/reduction are displayed here. As in SFC, the RDE CVs confirm a slight difference in Pd-oxide formation onset potential in the two electrolytes due to the diverse anion adsorption [1].

2.1 Poly-Pd reduction peaks with UPL

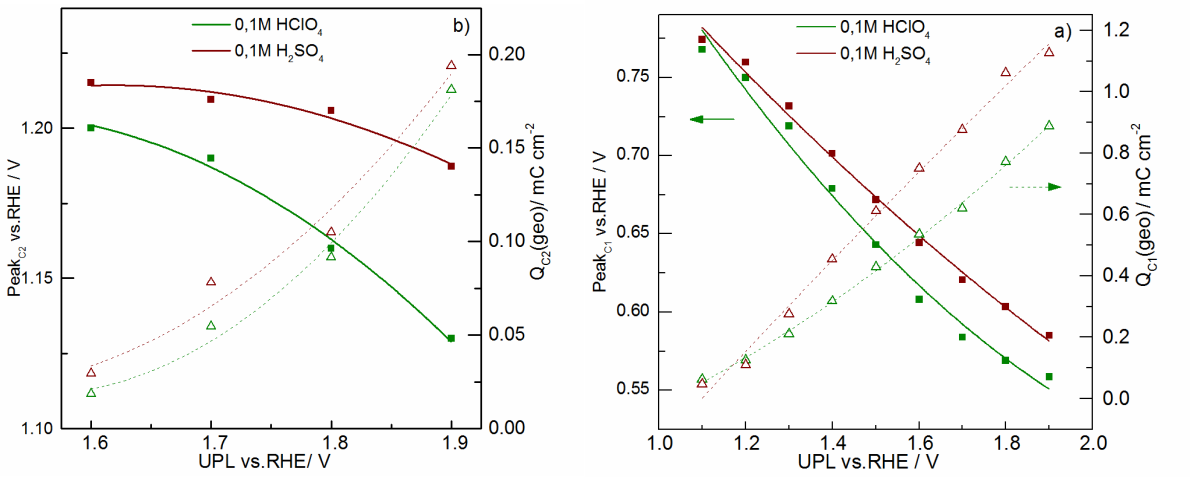

Figure S2.1 (a) Plots of peak potential $Peak_{C1}$ a charge density Q_{C1} of the Pd(II) reduction peak (C_1) as a function of the UPL. (b) Plots of peak potential Peak C_2 a charge density Q_{C2} of the Pd(IV) reduction peak (C_2) as a function of the UPL. Both

plots correspond to the poly-Pd cyclic voltammograms in perchloric and sulfuric acid shown in Figure 2.

The maximum reduction peak potentials and the calculated charge densities (corresponding to the cathodic scans of the CVs in Figure 2a) of the Pd(II)-oxide reduction peak (C_1) and of the Pd(IV)-oxide reduction peak (C_2) are shown in Figure S2.1. In the literature it is known that increasing the UPL the reduction peak of Pd is shifting to lower potentials as a direct consequence of the different amount of oxide formed[2], even though a clear explanation is not available at present.

In the case of Pd(IV)-oxide reduction peak no big difference is observed in the two electrolyte, whereas the position of the Pd(II)-oxide reduction peak in perchloric acid is shifting more to lower potentials compared to the shift in sulfuric acid. In fact, while with an UPL of 1.0 V_{RHE} no difference was observed in the two electrolytes, at much larger UPL the difference in the peak potential increases to almost 50 mV. Similarly the associated Pd(II)-oxide reduction charge is initially the same, while at higher potentials a difference up to ca. 20% in the reduction charge (higher in sulfuric acid) was measured (Figure S2.1). This is probably due to the different interaction of the electolytes anions with the Pd electrode (see discussion).

2.2 Poly-Pd potentiostatic passivation

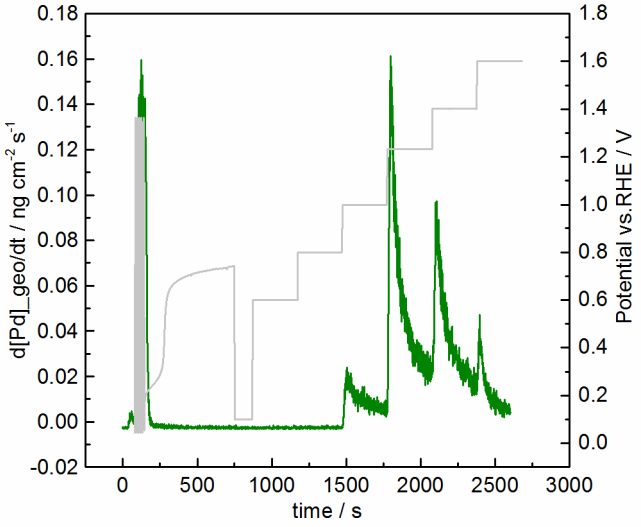

Figure S2.2 Potentiostatic dissolution of poly-Pd at different applied potential during a potential step experiment (time of each potential step: 300 s).

In Figure S2.2 is reported a measurement of the potentiostatic (steady-state) poly-Pd dissolution. The potential program applied consisted in 30 activation cycles followed by OCP and a series of potential steps of 300 s each with increasing potential from 0.6 to 1.6 V_{RHE} (0.2 V for each step). Dissolution is initially observed with potential of 1.0 V_{RHE}. For each step is observed a jump in dissolution, followed by a fast decay, indicating that there is no continue steady-state dissolution. Indeed, with time the oxide is covering and thus passivating the metal surface, resulting in the observed decrease in the dissolution.

3 Poly-Pd dissolution onset potential

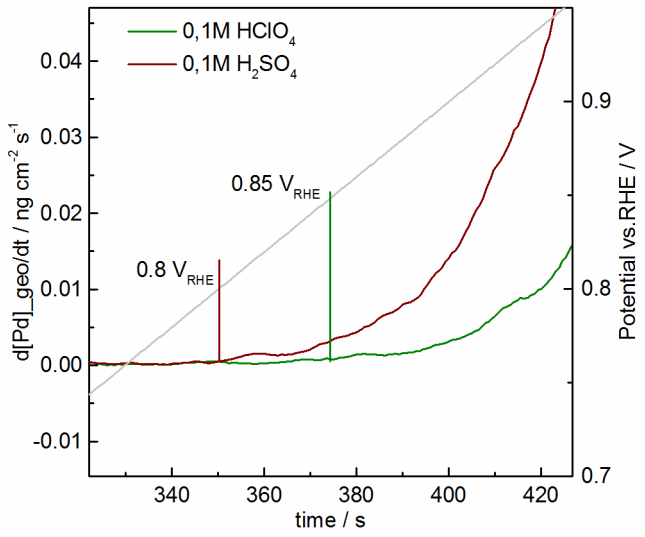

Figure S3 Comparison of the poly-Pd dissolution onset potential. Scan rate (2 mV s^{-1}).

In Figure S3 is shown a magnification of the poly-Pd dissolution signal collected by the ICP-MS during a positive-sweep at very low scan rate (2 mV s^{-1}). The Pd onset potential is evaluated as the deviation from the background signal. In the two electrolytes, the measured onset potentials appear shifted of approximately 50 mV. This might also be caused by the difference in the dissolution rates of Pd in the two analyzed electrolytes. Indeed, Pd in perchloric acid might also dissolve earlier than measured, but just being below the ICP-MS detection limit.

4 Poly-Pd dissolution at lower scan rate

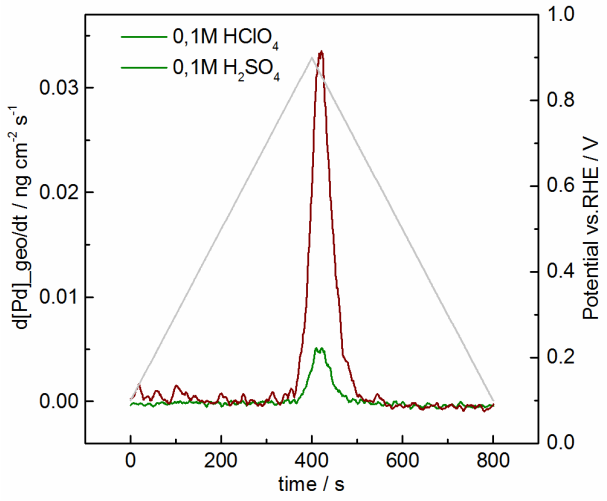

Figure S4.1 Poly-Pd dissolution profiles in 0.1M $HClO_4$ and H_2SO_4 with UPL= 0.9 V_{RHE}. Scan rate: 2 mV s^{-1}.

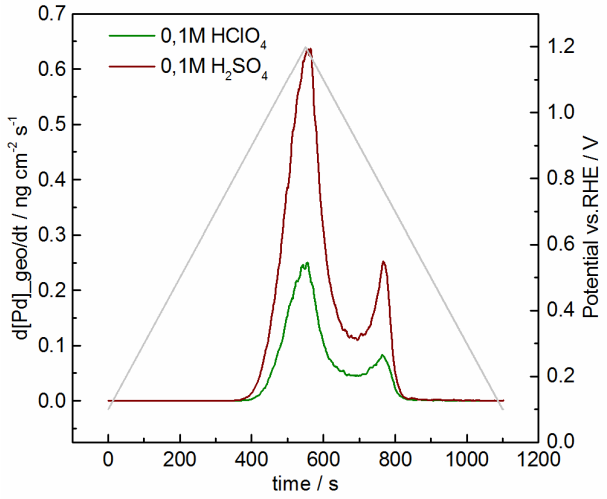

Figure S4.2 Poly-Pd dissolution profiles in 0.1M $HClO_4$ and H_2SO_4 with UPL= 1.2 V_{RHE}. Scan rate: 2 mV s^{-1}.

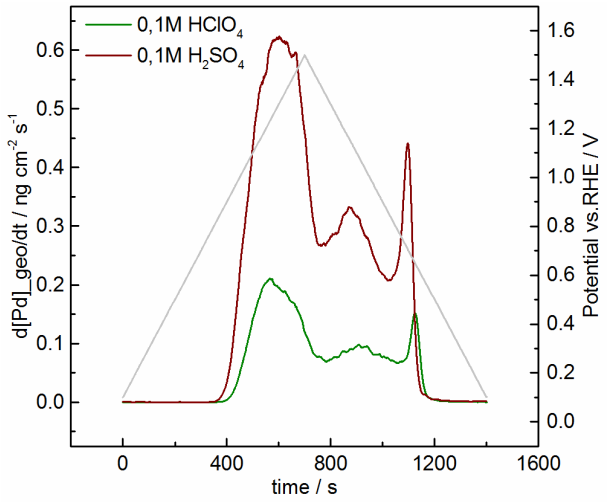

Figure S4.3 Poly-Pd dissolution profiles in 0.1M $HClO_4$ and H_2SO_4 with UPL= 1.5 V_{RHE}. Scan rate: 2 mV s^{-1}.

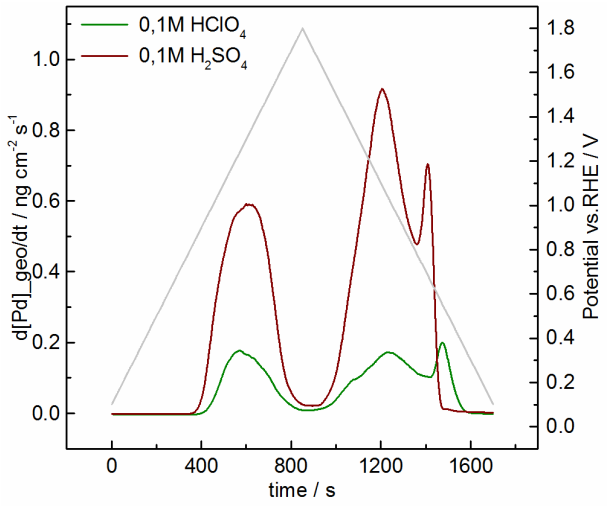

Figure S4.4 Poly-Pd dissolution profiles in 0.1M $HClO_4$ and H_2SO_4 with UPL= 1.8 V_{RHE}. Scan rate: 2 mV s^{-1}.

In Figure S4.1-4 are shown separately the four CVs and relative dissolution profiles corresponding to the measurement displayed in Figure 3. The difference in onset potential is once again evident for the different measurement. The maximum of the anodic dissolution peak in the two electrolytes matches very well for all the different UPL, whereas the maximum of the cathodic Pd dissolution peaks, in particular the peak C_1 are delayed with increasing UPL in the case of perchloric acid. This delay mirrors the greater shift of the Pd(II)-oxide reduction peaks with UPL observed in the CVs recorded in perchloric acid (Figure S2.1).

The quantitative difference between dissolution in perchloric and sulfuric acid, observed at faster scan rate (Table 1) is here confirmed (Table S4.1), even though in the case of slower scan rates the difference appears to be slightly reduced (the dissolution in sulfuric acid is here only almost 3 times than in perchloric acid, while at faster scan rate is 5 times).

Table S1 The comparison of amount of Pd in 0.1M H_2SO_4 and Pd* in 0.1M $HClO_4$ dissolved per cycle depending on the applied UPL as derived from potential sweep experiments at 2 mV s^{-1}.

UPL / V_{RHE}	Pd / ng cm_{geo}^{-2} $cycle^{-1}$	Pd* / ng cm_{geo}^{-2} $cycle^{-1}$
0.9	1.5	0.06
1.2	98.8	36.9
1.5	259.6	80.8
1.8	429.6	106.3

5 Poly-Pd mass CVs

In Figure S5.1 are shown the mass cyclic voltammograms corresponding to the poly-Pd dissolution profiles shown in Figure 3. The arrows indicate the positive and negative scan for the Pd mass cyclic voltammograms with 1.8 V_{RHE} UPL. The cathodic dissolution maxima are shifting to lower potentials with increasing UPL, accordingly to the thickness of the formed Pd oxide and thus to the shift in reduction peak [2].

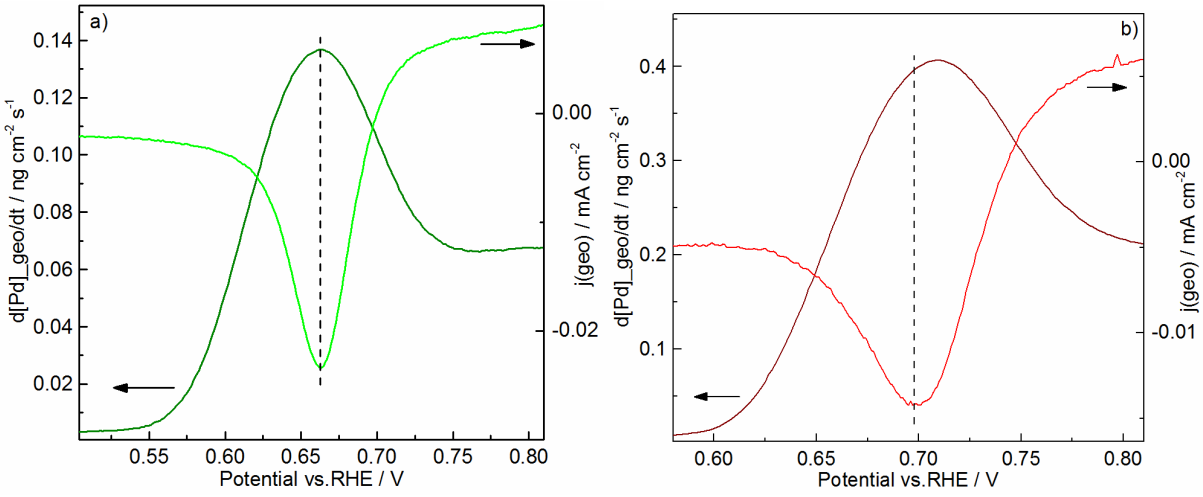

Figure 5 Correlation between cathodic dissolution and Pd(II)-oxide reduction signals in perchloric (a) and sulfuric acid (b). UPL: 1.5 V_{RHE}. Scan rate: 2 mV s^{-1}.

6 Pd/C

From the statistical average particle size and the loading a total initial surface area per printed layer of 0.31 mm^2 is calculated (A_s in Table S2).

	median / nm	mean / nm	st. dev.	ECSA* / m^2 g^{-1}	A_s (1l)** / mm^2
Pd	3.7	4.0	±1.3	124	0.31

*ECSA refers to the catalyst specific surface area, that was calculated from the particle mean size; **A_s refers to the total surface area of per deposited layer (≈2.5 ng)

Table S2 Particle size and specific surface area of the Pd/C catalyst investigated in

The surface area of the Pd/C nanocatalyst is estimated from the TEM average sizes following the calculation described in [2]. In our case a spherical geometry was assumed, whose volume is:

$$V=4/3\ \pi\ r^3 \qquad S1.1$$

Where r is the radius (half of the mean particle size as in Table S2).
The surface area is:

$$A=4\ \pi\ r^2 \qquad S1.2$$

Thus, the specific surface area is:

$$ECSA=3/(r*\rho) \qquad S1.3$$

Where ρ is the crystallographic density of palladium (ρ_{Pd}=12.02 g cm^{-3}):
The total metal surface area was calculated as follow:

$$A_s=ECSA*m \qquad S1.4$$

Where m is the mass of metal (2.5 ng_{metal})

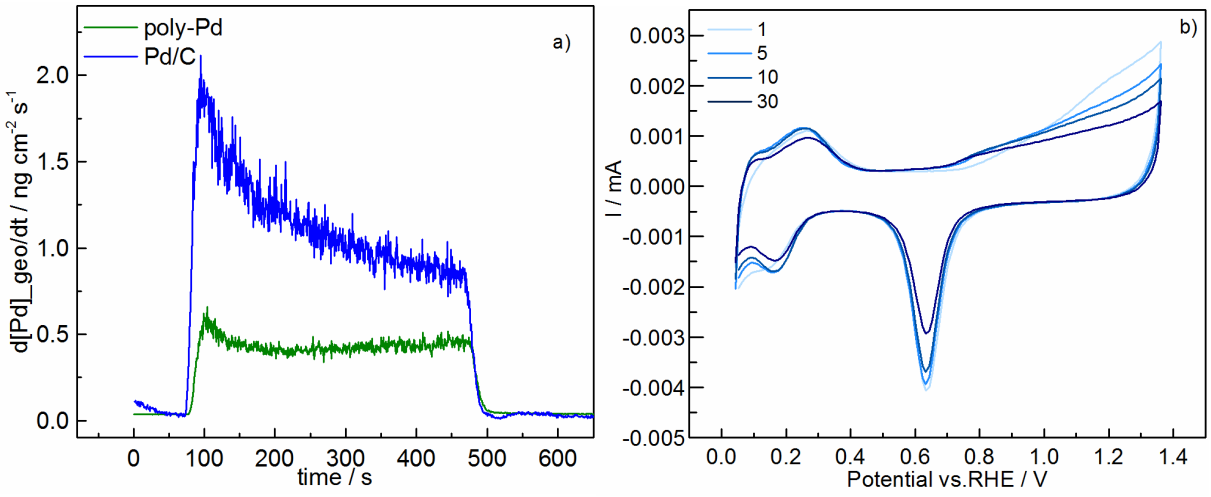

Figure S6.1 Dissolution profiles of poly-Pd and supported Pd/C nanoparticles during 30 activation cycles with a scan rate of 200 mV s^{-1} (a) and the corresponding cyclic voltammograms of the Pd/C electrode (b) in SFC. The Pd/C dissolution signal was normalized with the surface area after activation.

The CVs of the activation cycles and the associated dissolution are shown in Figure S6.1. In contrast with poly-Pd the dissolution rate of Pd/C is steadily decreasing. This is due to the fact that, unlike for bulk material, the dissolution of nanoparticles along with other degradation mechanisms lead to a decrease in surface area, evident from a comparison between the first and the last CVs of the activation protocol (Figure S6.1 b). Note that the dissolution profile for Pd/C has been normalized with the surface area of the last activation cycle that corresponds to the initial TEM area minus the difference in the Pd oxide reduction peak (decrease of the total surface area of approximately 35%).

The poly-Pd and Pd/C last activation cycles were also compared (Figure S6.2). The Pd/C reduction peak is much lower than that of poly-Pd (0.00148 and 0.00460 mC respectively).

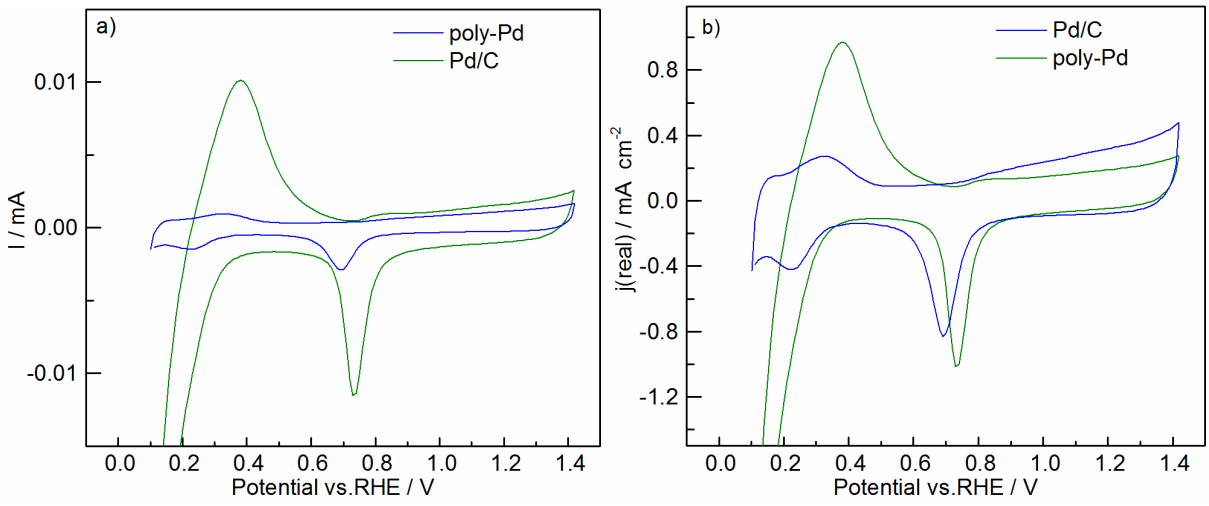

Figure S6.2 Last CVs of the activation cycle taken on a poly-Pd and Pd/C electrode in the SFC setup (normalized in b). Scan rate: 200 mV s^{-1}.

Table S3 Calculated charges of Pd-oxide reduction peaks and corresponding calculated areas using 424 µC cm^{-2} as reduction charge per unit area.

CV	Charge (µC)	Area (cm^2)
Initial Pd/C	2.28	0.0054
Activated Pd/C	1.48	0.0035
Activated poly-Pd	4.6	0.0109

[1] T. Solomun, The Role of the Electrolyte Anion in Anodic-Dissolution of the Pd(100) Surface, J Electroanal Chem, 302 (1991) 31-46.

[2] M. Grdeń, M. Łukaszewski, G. Jerkiewicz, A. Czerwiński, Electrochemical behaviour of palladium electrode: Oxidation, electrodissolution and ionic adsorption, Electrochim Acta, 53 (2008) 7583-7598.